

Registration and analysis of in-vivo multi-spectral images for correction of motion and comparison in time

Herke Jan Noordmans^{*a}, Rowland de Roode^a, Marius Staring^b
Rudolf Verdaasdonk^a

^aDept. of Clinical Physics and ^bImage Sciences Institute, University Medical Center Utrecht, Heidelberglaan 100, 3584 CX Utrecht, The Netherlands.

ABSTRACT

In-vivo image-based multi-spectral images have typical problems in image acquisition, registration, visualization and analysis. As its spatial and spectral axes do not have the same unit, standard image algorithms often do not apply. The image size is often so large that it is hard to analyze them interactively. In a clinical setting, image motion will always occur during the acquisition times up to 30 seconds, since most (elderly) patients often have difficulty to retain their poses. In this paper, we discuss how the acquisition, registration, display and analysis can be optimized for in-vivo multi-spectral images.

Keywords: Image registration, hyper-spectral imaging, dermatology, medical treatment tracking.

1. INTRODUCTION

In contrast to spectral measurements at one point, multi-spectral images measure the spectrum for an entire image. By moving the filter wheel of an electronically tunable filter, images are captured at a series of wavelengths. This results in a data stack with two spatial axes, x and y, and one spectral axis, λ (Figure 1). Such multi-spectral images have the advantage over point measurements that the spectrum is captured for all pixels in the image at the same time. Also, compared to images taken at a distinct set of wavelengths, multi-spectral images have the advantage that the full spectrum is available with high resolution. Multi-spectral imaging is used in e.g. microscopy and darkfield imaging, where it is applied to un-mix complex mixtures of fluorescent probes (<http://www.cri-inc.com>), or in satellite imaging where agricultural areas are monitored. In medicine, there are a few examples, e.g. the mapping of cancerous lesions of the cervix¹, and demarcation of brain tumors². Limiting factors for applying multi-spectral images in medicine are the demand for sterility, compact design, easy and fast usage to limit the interference with the workflow. A major problem working with patients is the motion during the acquisition time up to 30 seconds, introducing image motion artifacts. In this paper we will discuss the technical challenges and the solutions we developed to tackle these problems in applying a multi-spectral image system in a clinical environment. The process of multi-spectral imaging is split in subsequent steps: acquisition, registration, display and analysis. These steps are followed in the coming sections.

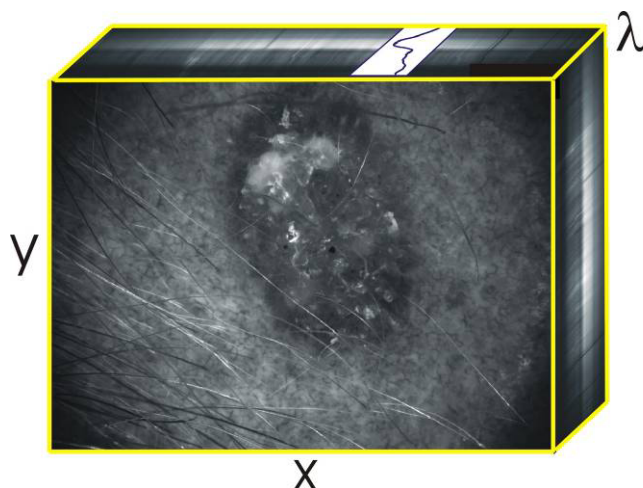


Figure 1 Multi-spectral image cube showing pre-cancer site Keratosis actinica (dermatology).

2. IMAGE ACQUISITION

Our multi-spectral camera consists of tunable filter of Cri type VariSpec VIS-10-20-STD (www.cri-inc.com, 400-700 nm, 10 nm bandwidth) and a high resolution 12-bit camera (PCO Pixelfly QE, www.pco.de). In front of the camera different lenses can be placed for specific applications. In a specially designed dermatoscope configuration, multi-spectral images can be obtained of the skin to track laser treatments or skin diseases^{3, 4}(Figure 2, top row). For neurosurgery, images can be made of the human cortex by mounting the multi-spectral camera on a surgical microscope made by Zeiss using a specially designed C-mount Zeiss adaptor (Figure 2, bottom row).

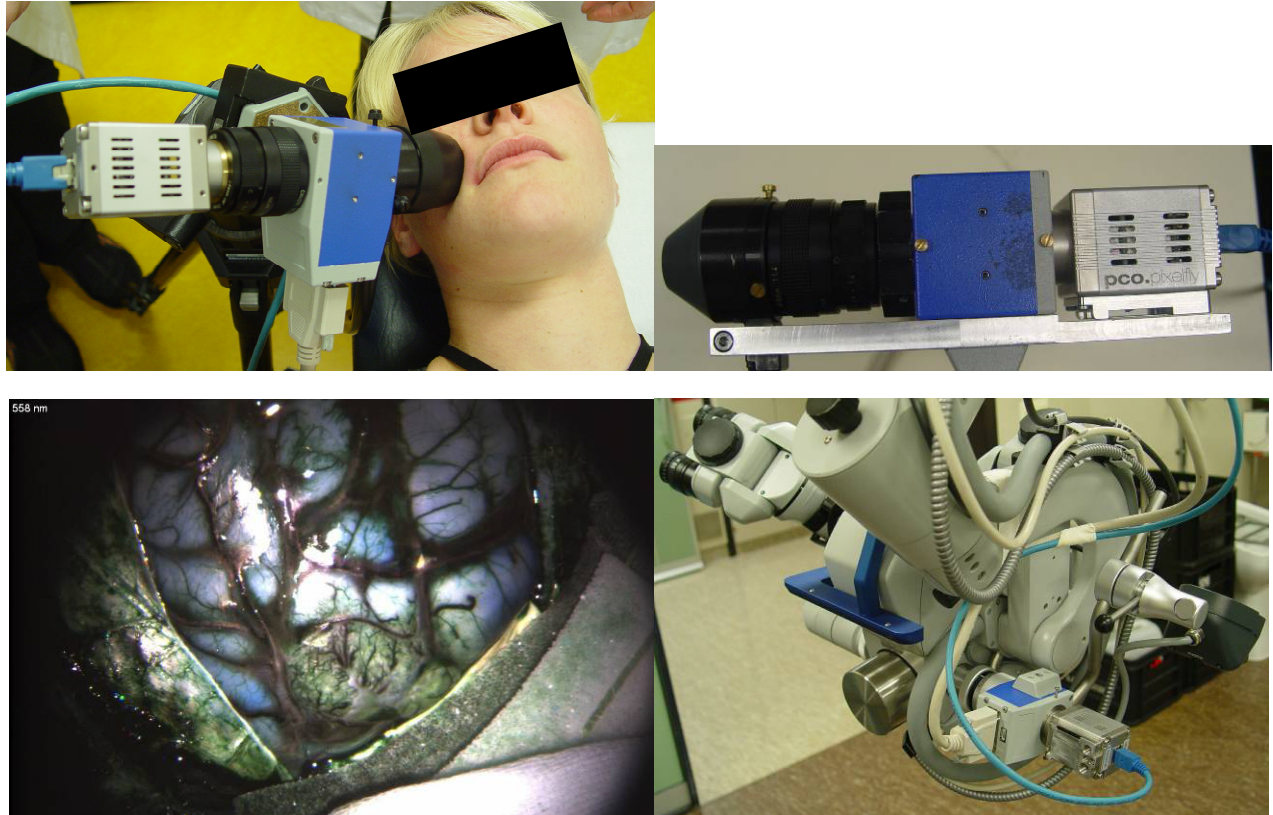


Figure 2 Multi-spectral imaging system adapted for use in dermatology (top row) and neurosurgery (bottom row). Note that using false colors for red (572 nm), green (490 nm), and blue (456 nm) the tumor outline in the lower-left image gets more pronounced.

3. IMAGE REGISTRATION

In contrast to multi-spectral images made of static objects like plants or microscope slides, patients tend to move while capturing a multi-spectral image (Figure 3). Although motion may be reduced by pressing the camera tighter on the skin of the patient, this is not preferred since the pressure limits the blood supply, causing interference with blood perfusion and consequently the results. In neurosurgery, the brain moves during the image capture sequence as a result of pressure changes during the breathing cycle of the patient. Matching of images is also required to compare images captured at different moments in time. For the application in dermatology, we developed a tool to reposition the dermatoscope roughly above the same location on the skin using real-time capture preview and overlay with the previous image. However, small misalignments remain which disturb further analysis.

To correct for image motion, we looked at image registration algorithms. Such algorithms are used in different fields, like radiology, to match images of the same or different modalities like CT, MR, PET, and SPECT⁵. The difference with multi-spectral images is that images from radiology are matched in three dimensions, while multi-spectral images are matched slice-by-slice. In addition, rigid matching often suffices in clinical practice, with three parameters, shift in x-direction, shift in y-direction, and rotation. However, with in-vivo multi-spectral images, rigid registration is often not sufficient as the tissue can elastically deform. Therefore, we need an elastic registration algorithm as illustrated in an example (Figure 4). At the top row, two images are shown which are taken of a 1 cm² area near the nose with a 2 day interval. The main image movement is in x-direction. Rigid registration results in the images of the second row, where the translation in the x-direction, and a small rotation, largely have been corrected. At first sight, the registration result looks almost similar to the reference image, but when image subtraction is applied, motion artefacts are still visible left and right to the main blood vessel. Elastic registration gives a better result as can be seen at the bottom row. The ‘zero difference’ or black area around the blood vessel is larger compared to the rigid registration, however image motion is visible near the corners. Parameter tuning may help to give a better registration result, but there will often be areas where there is too little surface detail for the registration algorithm to get a correct registration result.

A drawback of applying elastic registration is the many parameters which need to be optimized. The time for registering two multi-spectral images elastically takes often 25 times longer than matching the images using rigid registration. In our case of matching two images of size 1392x1024 the elastic match takes nearly 4 minutes on a 3GHz PC, while the time for a rigid match is only 10 seconds.

Apart from the problem of matching two spectral images, it is important which strategy is used in matching all the images in one multi-spectral dataset towards each other. As an image taken near UV differs maximally from that taken near IR, the simplest approach is to match all images to the image taken at the central wavelength (Figure 5a). Still, the difference between two images may be too large for a good match. Another strategy may be to match images to their spectral neighbors, see Figure 5b. As differences between two consecutive images are small, matches will probably not fail. However, as match errors will probably propagate, it will still be a problem to match images at the ends of the spectral series. Therefore, a better strategy might therefore be to split the spectral range in different blocks, where each image is matched to the image at the central wavelength of its block and these central images again towards each other (Figure 5c).

As the difference after employing these registration strategies may still be too large, it can even be better to adapt the scanning sequence to the registration strategy (Figure 6). By first scanning the spectral range coarsely and afterwards with finer steps, large differences due to motion between matched images can be prevented.

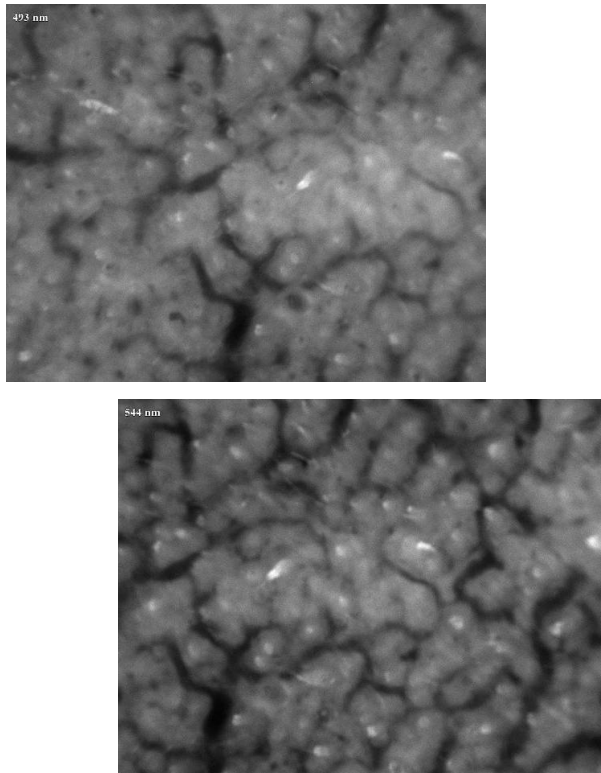


Figure 3 Example of large (horizontal) image motion during acquisition of multi-spectral image in dermatology.

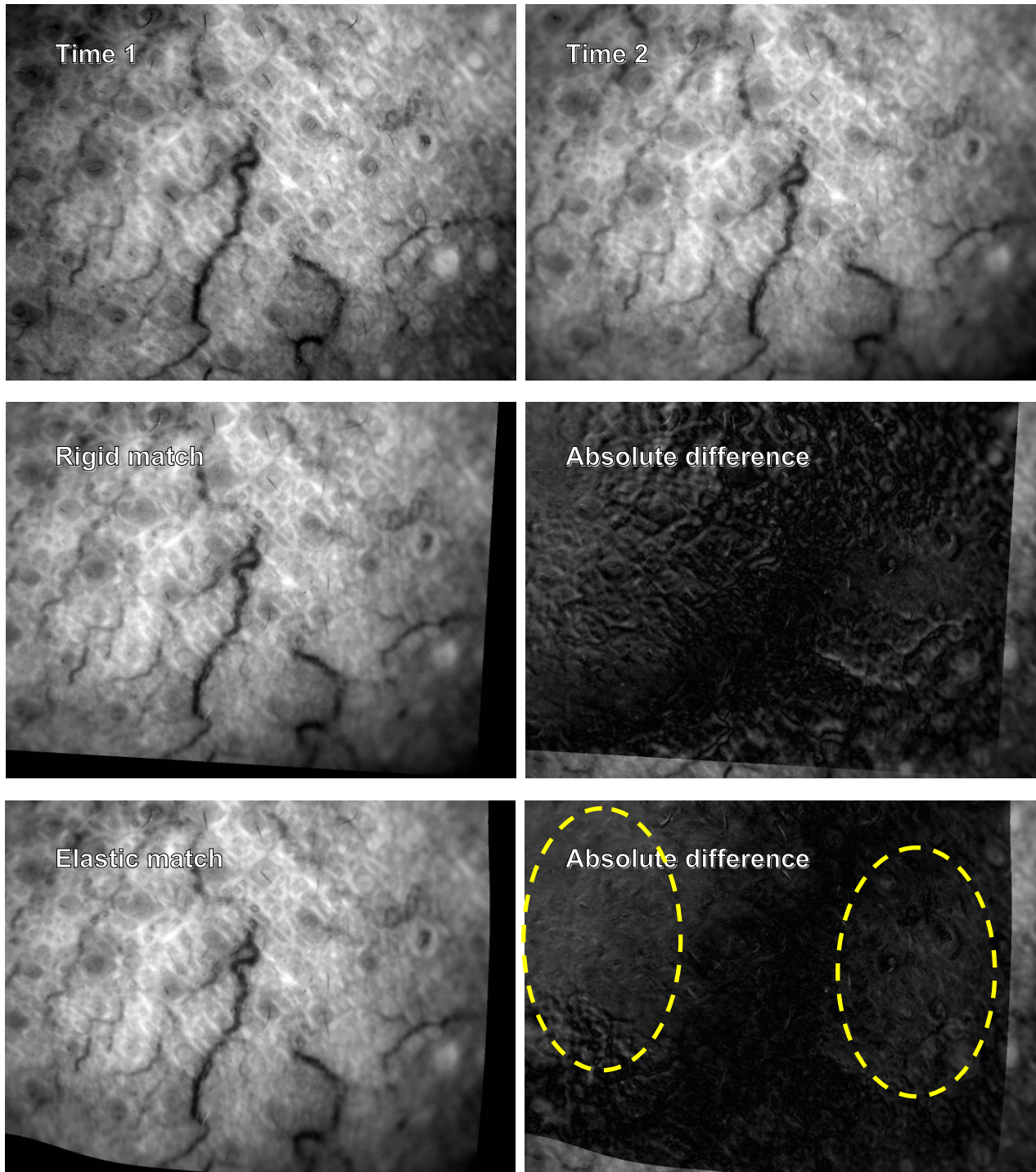


Figure 4 Comparison of rigid and elastic matching methods. Top row: Two spectral images taken of area near the nose two days after each other. Second row: Result of rigid matching. Global motion has largely been corrected. Bottom row: Result of elastic matching. More fine details have been corrected. Note the errors denoted by the ellipses where there was not enough information for a correct match.

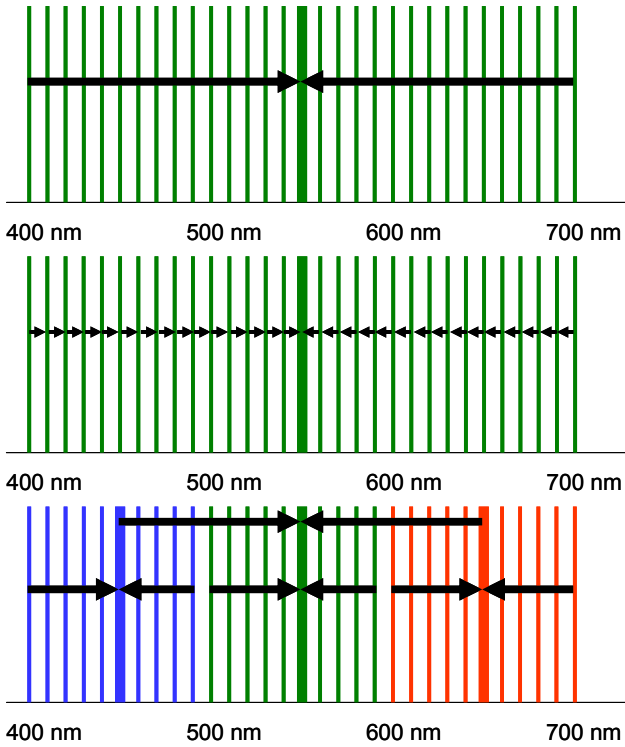


Figure 5 Different spectral matching strategies. Top: Match images to the image at the central wavelength. Middle: Match images to their predecessor. Bottom: Match images in sets of which the center images are matched to the image at the central wavelength.

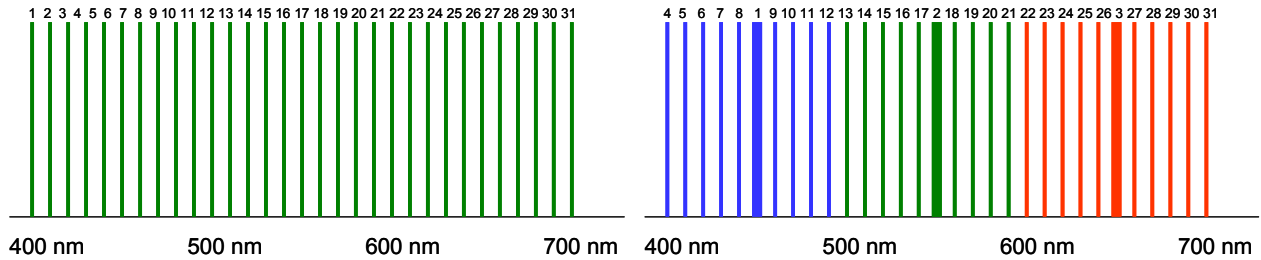


Figure 6 Scanning strategy optimized for matching spectral images. Left: Conventional strategy of matching all wavelengths sequentially. As the scan takes about 30 s, significant motion may have occurred at the end of the sequence. Right: Scan coarsely but fast through the spectral range with less motion artefacts and scan more detailed wavelengths afterwards.

4. IMAGE DISPLAY

The display of multi-spectral images can be done in several ways. As all image data cannot be perceived at once, there is no perfect method. In our software, several display methods are present to cover the user's needs:

1. Image browsing through the spectral range to see all spectral images (Figure 7).
2. Pseudo color images by combining spectral images into the red, green and blue spectral bands (RGB) of a color picture. Such an image resembles a poor color photograph due the small-band nature of a multi-spectral image set. A better correspondence is acquired by simulating the sensitivity curves of the human eye by integrating the images over the spectral range.
3. Contrast stretching as multi-spectral images can have a high dynamic range (with our camera 12-bits) which needs to be compressed before it can be displayed on an 8-bit screen. Automatic min-max stretching methods often fail as noise or high-lights influence the extreme value in a stochastic way by which image stretching becomes a matter of chance. A better way is to remove the outliers by binning the image data into a histogram and determining the minimum and maximum from the 1% and 99% percentile (or other percentages if they appear better).
4. Image algorithmic to enhance tissue characteristics or calculate tissue concentrations from images at different wavelengths. Simple techniques are image subtraction and image division (ratio analysis).
5. Image comparison to track diseases or treatments. One can place multi-spectral images take at different moments in time side-to-side to compare them visually. Comparison can again be enhanced by subtraction or division (ratio imaging).
6. Display of full spectrum at a pixel to show the reflection spectrum at the tissue location of interest. The spectra of several pixels can be grouped to increase the signal noise ratio. Differences between spectra can be enhanced by subtracting or dividing two spectra (Figure 8).

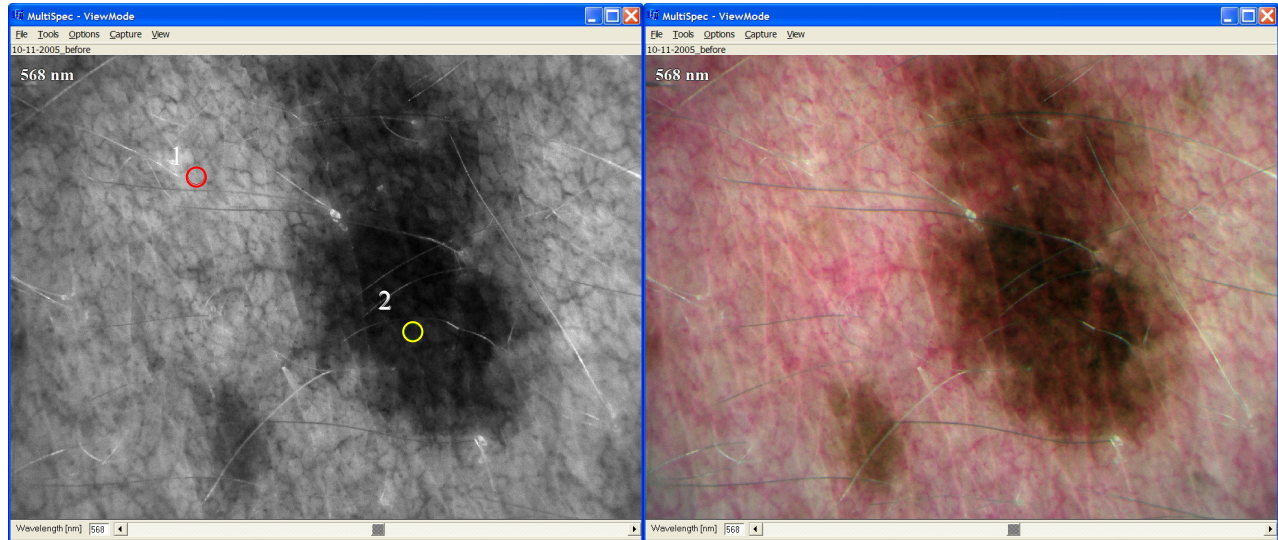


Figure 7 Normal and pseudo color display.

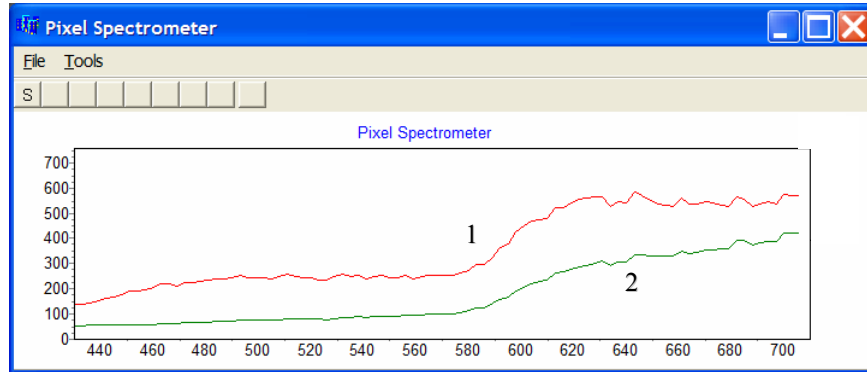


Figure 8 Pixel spectrometer given the reflection spectra for the circles in Figure 7.

5. IMAGE ANALYSIS

In the clinical environment, the previous steps are crucial before any image analysis and interpretation can be performed. The observer needs to have a good insight in the way the images were acquired and which information is embedded that can be abstracted, before any image analysis tool can be applied. Once these steps are performed satisfactory one could think of different algorithms to aid the clinician with interpreting the results. One option to help the clinician with the diagnosis could be to segment the image into an ‘interesting object’ and a non-interesting background⁶. This can be done by thresholding the pixel values, directly or after pre-filtering the data in the image or spectral domain. Examples of such filters are de-noising filters like a Gaussian filter, edge detection filters, line detection filters, etc. Another option would be to classify the image using features from the image and spectral domain. Examples of such algorithms are k-nearest neighbor classification, principal component analysis or independent component analysis⁷.

There are many algorithms suited for analyzing multi-spectral images in either the image or the spectral domain. However, only a few algorithms make efficiently use of both domains. The best approach so far is to put features from both the image domain and the spectral domain into a feature vector which can subsequently be used in the classification process. Still the problem with such classification algorithms is which features to use. The more features are used, the better the classification of the test set will be in general, but also the computation time will increase dramatically. A classification algorithm which automatically selects the strongest features is reported in literature for the analysis of multi-spectral histology slides in pathology⁸.

6. SOFTWARE IMPLEMENTATION

Multi-spectral image data sets can be very large, for example, 300 spectral images with a resolution of 1392x1024 and 2 bytes per pixel results in a file of 800 MB. For time series, the file size can even extend beyond the 4GB limit of 32bit operating systems. To analyze such a large file interactively, the software needs special adaptations. We developed a solution to access the multi-spectral image file in pieces as it cannot be fully loaded into memory anymore. This is done by mapping the interesting part of a multi-spectral image file to the memory space of the program (Figure 9). To know which parts of the file need to be mapped, image procedures are preferably split into line operations, either in x-, y- or λ -direction. Such a line is then mapped into memory after which the image algorithm can process that line. By using memory mapped files the operating system itself takes care of reading the pixel bytes from file and writing them back if they have changed. In this way the opening of a file requires only the read of a few slices and can be accomplished in a few seconds. Only more slices are read when this is needed. Note that 64 bit operating systems are the preferred over 32 bit operating systems as much larger files can be directory mapped to memory space (15 million TB files versus 2 GB files), thereby bypassing the need to explicitly control which part of the file is addressed.

Another characteristic of our software is the use of a cubic pixel layout to optimally use the processor cache when processing the image in the spectral dimension λ , see Figure 10. One line in memory then first consist of 8 pixels in x-

direction (denoted by circle 1), then 8×8 pixels in y-direction (circle 2) and finally $8 \times 8 \times 8$ pixels in λ -direction for one cube (circle 3). This is repeated for all cubes in x-direction (circle 4), y-direction (circle 5) and λ -direction (circle 6). Compared to a linear pixel layout, some performance loss in the x- and y-direction is traded for 8-fold performance gain in λ -direction, which is especially needed to show the spectrum of a region of interest.

Patient motion requires the image to be captured as fast as possible. This is achieved by using a light efficient camera, using pixel binning where high spatial resolution is not needed, and using the highest illumination power possible. Previews of the captured images should be displayed with DirectDraw or Direct3D and not with GDI (all of Microsoft) to efficiently exploit the optimizations of the graphic processor. On a 3 GHz processor system, this makes the difference between a preview rate of 8 frames per second and 60 frames per second on a normal graphic card.

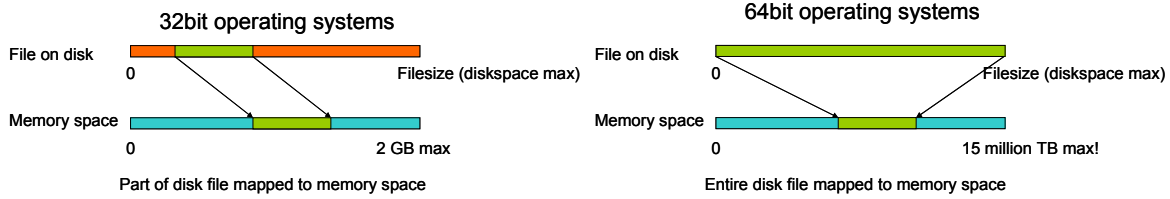


Figure 9 Intelligent memory mapping large image files for 32 bit or 64 bit operating system. In this way, large multi-spectral image data (>1 GB) can be displayed in two seconds.

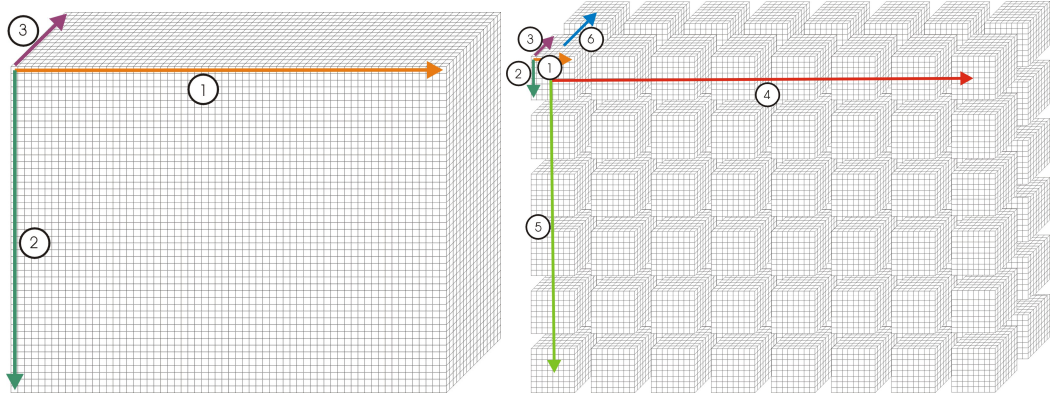


Figure 10 Pixel layout options for multi-spectral images. Left: Linear layout for fast access in x- and y-direction, but not in λ -direction. Right: Cubic pixel layout for (somewhat less) fast access in x-, y-, direction but 8-fold faster access in λ -direction.

7. CONCLUSIONS

Multi-spectral imaging of in-vivo tissues in clinical settings requires additional demands in image acquisition, registration and analysis. Scanning and registration strategies have been developed to counter the problem of image motion during the image capture process. Additional system and software strategies have been developed to handle large multi-spectral images in an interactive way. The proposed techniques will make multi-spectral imaging systems more accessible for practical use and acceptance in clinical settings.

REFERENCES

1. C. Balas, *A novel optical imaging method for the early detection, quantitative grading, and mapping of cancerous and precancerous lesions of cervix*, IEEE Trans Biomed Eng. 48(1), 2001, pp. 96-104.
2. S.C. Gebhart, W.C. Lin, A.M. Mahadevan-Jansen, *Characterization of a Spectral Imaging System*, Proc. SPIE Int. Soc. Opt. Eng. 4959, 2003, pp. 34-45.
3. H.J. Noordmans, R. de Roode, and R.M. Verdaasdonk, *Development of a multi-spectral imaging system for optical diagnosis of malignant tissues*, Proc. SPIE Int. Soc. Opt. Eng. 5694, 1, 2005, pp. 1-8.
4. R. de Roode, H.J. Noordmans R.M. Verdaasdonk, A. de Laheije, *Reproducible multi-spectral imaging in dermatology for diagnostics and treatment evaluation*, Proc. SPIE Int. Soc. Opt. Eng., 6078A-28, 2006.
5. D. Rueckert, L.I. Sonoda, C. Hayes, D.L.G. Hill, M.O. Leach, and D.J. Hawkes, *Non-rigid registration using free-form deformations: application to breast MR images*, IEEE Transactions on Medical Imaging 18 (8), 1999, pp. 712-721.
6. H.J. Noordmans, R. de Zeeuw, R.M. Verdaasdonk, C.H. Wittens, *Infrared imaging of varicose veins*, Proc. SPIE Vol. 5325, 2004, p. 157-163.
7. G. Polder, *Spectral imaging for measuring biochemicals in plant material*, PhD thesis TU Delft, 2004.
8. J. Zhang and Y. Liu, *Cervical Cancer Detection Using SVM Based Feature Screening*, Proc MICCAI '04, Vol. II, 2004, pp. 873 – 880.